Multifractal geometry in stock market time series

Antonio Turiel [1]

Air Project - INRIA.
Domaine de Voluceau BP105. 78153 Le Chesnay CEDEX
France.

Conrad J. Pérez-Vicente *

Grup de Sistemes Complexos.
Departament de Fisica Fonamental.
Universitat de Barcelona. Diagonal, 647.
Barcelona 08028.Spain.

Abstract

It has been recently noticed that time series of returns in stock markets are of multifractal (multiscaling) character. In that context, multifractality has been always evidenced by its statistical signature (i.e., the scaling exponents associated to a related variable). However, a direct geometrical framework, much more revealing about the underlying dynamics, is possible. In this paper, we present the techniques allowing the multifractal decomposition. We will show that there exists a particular fractal component, the Most Singular Manifold (MSM), which contains the relevant information about the dynamics of the series: it is possible to reconstruct the series (at a given precision) from the MSM. We analyze the dynamics of the MSM, which shows revealing features about the evolution of this type of series.

Key words: Economics, business, and financial markets, Structures and organization in complex systems, Fractals
PACS: 89.65.GhE, 89.75.Fb, 05.45.Df

* To whom correspondence should be addressed
Email addresses: Antonio.Turiel@inria.fr (Antonio Turiel), conrad@ffn.ub.es (Conrad J. Pérez-Vicente).
[1] Also Laboratoire de Physique Statistique, Ecole Normale Supérieure de Paris

1 Introduction

The analysis of financial time series has been the focus of intense research by the physics community in the last years (1; 2). The aim is to characterize the statistical properties of the series with the hope that a better understanding of the underlying stochastic dynamics could provide useful information to create new models able to reproduce experimental facts. In a further step such knowledge might be crucial to tackle relevant problems in finance such as risk management or the design of optimal portfolios, just to cite some examples.

Another important aspect concerns concepts as scaling and the scale invariance of return fluctuations (3; 4). There is an important volume of data and studies showing self-similarity at short time scales and an apparent breakdown for longer times modeled in terms of distributions with truncated tails. Recent studies have shown that the traditional approach based on a Brownian motion picture (5; 6) or other more elaborated descriptions such as Levy and truncated Levy distributions (2), all of them relying on the idea of additive process, are not suitable to properly describe the statistical features of these fluctuations. In this sense, there are more and more evidences that a multiplicative process approach is the correct way to proceed and this line of thought leads in a natural way to multifractality. In fact, this idea was already suggested some years ago when intermittency phenomena in return fluctuations was observed at different time scales which gave rise to some efforts to establish a link with other areas of physics such as turbulence (7; 8). Nowadays, we know that there are important differences between both systems, as for instance the spectrum of frequencies, but the comparison triggered an intense analysis of the existing data. The multifractal approach has been successful to describe foreign exchange markets as well as stock markets (9).

Multifractal analysis of a set of data can be performed in two different ways, analyzing either the statistics or the geometry. A statistical approach consists of defining an appropriate intensive variable depending on a resolution parameter, then its statistical moments are calculated by averaging over an ensemble of realizations and at random base points. It is said that the variable is multifractal if those moments exhibit a power-law dependence in the resolution parameter (10). On the other hand, geometrical approaches try to assess a local power-law dependency on the resolution parameter for the same intensive variables at every particular point (which is a stronger statement that just requiring some averages -the moments- to follow a power law).

While the geometrical approach is informative about the spatial localization of self-similar (fractal) structures, it has been much less used because of the

greater technical difficulty to retrieve the correct scaling exponents. However, in the latest years an important effort to improve geometrical techniques has been carried out, giving sensible improvement and good performance (11; 12). We will apply the geometrical approach in this paper as a valuable tool for the understanding of the geometry and dynamics of stock market time series.

The paper is organized as follows: in Section 2 the data are presented; then, Section 3 is devoted to the introduction of geometrical techniques; results of its application to our data are also shown. Section 4 provides an interpretation of the particular multifractals observed in the price series; we will see that those multifractals can be reconstructed from the information conveyed by a single fractal component. We apply the theory to our context and extract valuable conclusions about dynamics. A simple model for that dynamics is presented in Section 5, while the stability of the model with the observed data is discussed in Section 6. The conclusions of our work are then issued in Section 7.

2 Settings

We have processed two different kind of data belonging to the Spanish stock market (IBEX) which correspond to well different time scales. The first group is formed by daily series of 17 different assets (those with the largest liquidity) during approximately ten years (from January 1st, 1990 to May 24th , 2001) containing 48458 points. The second group consists of 12 month series (during 1999) for the 4 most important assets of the market, also included in Euro Stoxx 50, each series being sampled at a time interval of one minute containing 275477 points. For this group, there are clear, systematic disruptions at precise moments such as the opening of the local market or the opening of NY market (3:30 pm local hour), for instance. In spite of the fact that those events elicit statistical deviations from the multifractal model, they do not affect significantly to our calculations due to the high sampling rate. For that reason we do not try to correct the systematic deviations by any mean, performing the same analysis for the two groups. In the same spirit, we always identify the ending of a session as the instant just preceding the opening of the following, no matter the actual time interval between them (sometimes several non-working days) for both types of series. Examples of series of the two types are shown in Figures 1 and 2.

We are interested in relative variations of the price, i.e., the ratio of the absolute value to the absolute variation. For that reason, we will work on series formed by logarithms of prices. In such a way, the absolute variation between two consecutive instants (approximately, the derivative with respect to time)

for this series approximates the relative variation for the original stock series.

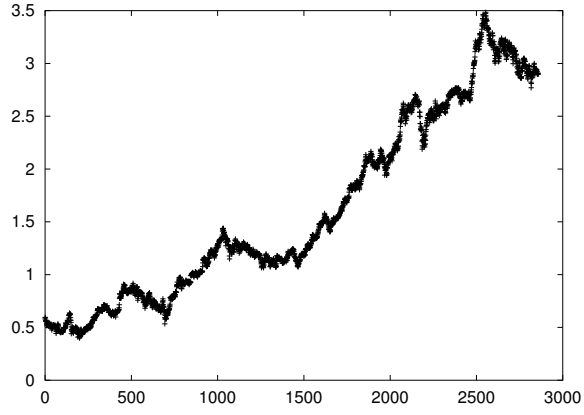

Fig. 1. Ten-year daily series of the log of prices for Telefónica (TEF)

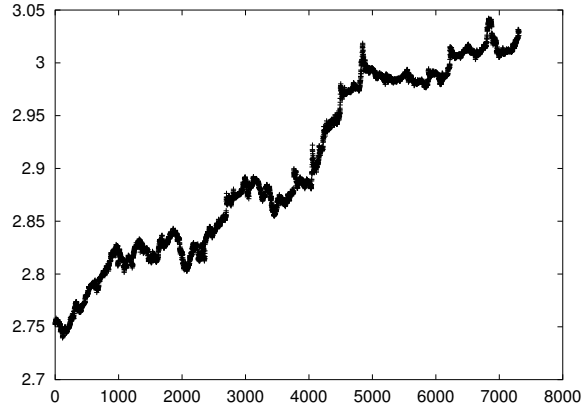

Fig. 2. November 1999 minute series of the log of prices for Telefónica (TEF)

3 Multifractal analysis

3.1 Singularity analysis

Self-similar (or multifractal) signals are usually characterized by a very irregular behaviour: at some point they show very abrupt transitions while in points nearby the function behaves rather smoothly. Such systems are also scale invariant, what means that no statistical variable can depend on an inner scale: the process should seem the same when a change in scale is performed. Combining both principles (irregular distribution of transitions, scale invariance) it should be expected that the series $s(t)$ can be expanded around a given

instant t_0 as:

$$|s(t) - s(t_0)| \sim |t - t_0|^{\alpha_0} \tag{1}$$

The exponent α_0 is the so called singularity exponent or Hölder exponent (13) associated to t_0. Eq. (1) is of course scale invariant, and the smooth or irregular character of the transition at t_0 depends on value of α_0. The greater the exponent, the most regular the signal will be at that point.

It is expected that the value of the singularity exponents associated to the different instants vary greatly, in order to give account of the irregular nature of the series. To describe the series, it would be then convenient to calculate the singularity exponents at every time t, that is, to perform a singularity analysis of the series. The naif way to proceed is to test eq. (1) at every time t_0 and to calculate the function $\alpha(t_0)$ of singularity exponents. Singularity analysis thus generalizes the concept of Taylor expansion for irregular, chaotic signals.

Such a simple singularity analysis is rather standard in the study of turbulent flows, and it has been used in different studies of stock market series as well as in (10). However that definition of singularity exponent (eq. 1) is not well adapted for signals with constant contributions to the two-point correlation. This is the case for intermittent, locally non-stationary signals, in which fluctuations are long lived (14). In that case, the lack of stationarity masks the presence of positive singularity exponents, making them impossible to detect. There are two possibilities to overcome this difficulty: to build a stationary measure (as in (15)) or to project the signal over a wavelet basis (as in (16)). We will apply both techniques: the first, to create a stationary signal; the second, to provide a smooth way to interpolate data over discretized sampling.

It is well known in stock market series that price fluctuations are correlated only over very small time windows, while their absolute values correlate over very large time intervals with power law distribution (17; 18). Having this in mind, a stationary, power-law correlated measure can be defined from the absolute value of the variations of the series. The measure μ of an interval $[t, t']$ is given by:

$$\mu([t, t']) \equiv \int_t^{t'} d\tau \; |s'|(\tau) \tag{2}$$

where $s'(t)$ is the derivative of $s(t)$ with respect to t. This measure accumulates the absolute variations of the series over the given interval, so giving an idea of its irregularity. As absolute fluctuations are power-law correlated, it is reasonable to expect that the measure depends as a power law in the size

of the time window (10; 11). Singularity analysis can be performed now by computing the singularity exponents associated to this measure at any time t.

Systematic singularity analysis leads to the classification of points according to the value of the singularity exponents. Such a classification splits series in different invariant sets of fractal nature, and for that reason we speak about multifractality. We define here multifractal measures and we will discuss later the classification scheme. We will say that μ is multifractal if at any time t_0 there exists a singularity exponent h_0 such that:

$$\mu([t_0 - \Delta t, t_0 + \Delta t]) \ \sim \ \Delta t^{h_0+1} \tag{3}$$

for sizes Δt small enough. The parameter Δt plays the role of a resolution parameter: only relevant details at that temporal extent are detected. According to eq. (3), a multifractal measure has an associated singularity exponent at every point. As before, we expect the singularity exponent to change from one instant to another.

It is important to remark the structure of the measure given previously. The exponent is a sum of two terms: the dimension of the space, that for the time series discussed in this paper equals 1 (time), and the singularity exponent which is independent of dimensional considerations. By operating in this manner we can separate both contributions in a systematic way which is very convenient to deal with physical systems in different dimensions. Since the measure is a quantity with physical meaning, we expect to find $h(x) > -1$ to ensure continuity and avoid any divergence.

Over experimentally sampled data, eq. (3) is very crude and poorly operative to check multifractality. Singularity analysis is then usually done by means of an appropriate interpolation technique: that of wavelet projections. Given a wavelet Ψ (that is, a function verifying some appropriate conditions), the wavelet projection of μ at t_0 and scale Δt (denoted $T_\Psi \mu(t_0, \Delta t)$) is defined as:

$$T_\Psi \mu(t_0, \Delta t) \ \equiv \ \int d\tau \, |s'|(\tau) \frac{1}{\Delta t} \Psi(\frac{t_0 - \tau}{\Delta t}) \tag{4}$$

The measure μ is multifractal (in the sense of eq. (3)) if and only if the wavelet projections over a properly chosen wavelet Ψ at a given time t_0 verify:

$$|T_\Psi \mu(t_0, \Delta t)| \ \sim \ \Delta t^{h_0} \tag{5}$$

with exactly the same exponent (13; 12) h_0 as in eq. (3) [2] . Wavelets are necessary to provide a smooth interpolation over discretized data and to improve

[2] As a matter of fact, the exponent h_0 is not independent of the exponent α_0 in

the assess of the local behaviour in real, experimental situations [3] .

3.2 Multifractal decomposition

Once singularity exponents at every time t are known (which we will represent by the function $h(t)$, that is, $T_\Psi \mu(t, \Delta t) \sim \Delta t^{h(t)}$) it is possible to classify points according to common values of the exponents. We define the fractal component F_h associated to the singularity exponent h as the set of points verifying:

$$F_h \equiv \{ h(t) = h \} \tag{6}$$

Fractal components arrange together those points sharing the same scale invariance properties (the same scaling exponent). This multifractal decomposition provides a natural hierarchy for the series which is reflected on its statistical properties. Due to the irregular, chaotic character of the series, the sets F_h are truly fractal in nature (that is, they have non-trivial fractal dimensions). The geometry of those sets is rather informative about the underlying dynamics driving the series, as their arrangement is quite structured and highly non-trivial (we will return to that question in Section 4). An important quantity in multifractals is the function defined by the dimension of each fractal component. The singularity spectrum $D(h)$ of the multifractal is defined as the function given by the Haussdorf (or fractal) dimension of the component F_h,

$$D(h) \equiv \dim F_h \tag{7}$$

The singularity spectrum plays a crucial role in relating geometry (multifractal decomposition) and statistics (self-similar properties as those studied in (10)): the statistical self-similar exponents are obtained by a Legendre transform of the singularity spectrum (21). In that way, the geometry of such chaotic series

eq. (1) in the cases in which the later makes sense: it can be proven that $\alpha_0 = h_0 + 1$ (12).

[3] Wavelet projections also allow removing constant correlations: if a certain order of moments of the wavelet Ψ vanish, it could be used to directly analyze the series s instead of the measure μ (19; 12; 20). The drawback of such wavelets lies in that fact that they possess a complicated structure of zero-crossings, so the minimum resolution at which they can be used over a discretized sample is of the size of several sampling points. For that reason we have preferred working on the measure μ and using less structured, finer resolving wavelets.

is reflected in a power-law behaviour of the distribution of certain variables. The two concepts (geometry and statistics) are so intimately related that it is usual to talk about multifractality when just the statistical analysis has been performed. We will show that the geometrical approach provides a more precise picture of the dynamics of the series. For a discussion of the connection between the statistical and geometrical approaches, the reader is referred to (10) in the context of stock market time series, and to (11) for a more general analysis.

3.3 Experimental results

All the series were analyzed using several wavelets from the Laplacian family, $\Psi_\gamma(t) = (1 + t^2)^{-\gamma}$, with $\gamma = 1, 1.5, 2$. Such functions are not *admissible* wavelets, that is, they cannot be used to represent any particular series (13); they can be used however to perform singularity analysis on positive multifractal measures (12). Those particular wavelets provide a fine spatial localization at the cost of restricting the range of singularities which is possible to detect. Those functions are able to resolve all the effective range of singularities in log-Poisson multifractals, which is the case of the analyzed series (we will discuss log-Poisson multifractals in Section 4). The exponent $h(t)$ at every time t was computed as the slope of a log-log linear regression of the absolute value of the wavelet projection vs. the resolution Δt (see eq. (5)), for resolutions continuously sampled in the interval $[1, 3]$ (here the units are tics, i.e., number of points). In all the stock market series, for a vast majority of the points ($\geq 99\%$) the linear regression exhibited good regression coefficient (absolute value above 0.9), validating the multifractal framework. For details on wavelet singularity analysis the reader is referred to (12) and references therein.

The results obtained with the different wavelets are comparable. In Figure 3 we show a typical exponent function $h(t)$; as it is clearly seen, it is extremely irregular, chaotic in behaviour. It is thus not so surprising that the different fractal components are truly fractal in character. We had not tried to provide a representation of each fractal component, as they have a very complicated structure, difficult to decipher from a simple plot.

The experimental distribution of singularities showed that the possible values for the singularity exponents were in all the cases contained in a range included in $[-1, 2]$ (see Figure 4). There always existed a non-trivial, minimum value h_∞ verifying $-1 < h_\infty < 0$, as we expected. The existence of a finite lower bound in h is not surprising: the range of possible singularities is always bounded from below for finite variation series (that is, the series can be discontinuous,

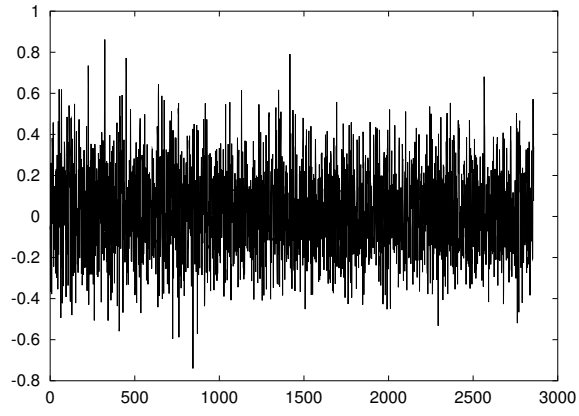

Fig. 3. Function $h(t)$ for Telefónica daily series (Figure 1). It is strongly irregular. Theory predicts that it is everywhere discontinuous (12), what is connected with the fact that its level sets (the fractal components) are of non-trivial fractal dimensions. The total discontinuity of $h(t)$ makes the fractal components to be strongly spatially correlated (randomly placed singularities would lead to some continuity points). For that reason, contrary to intuition multifractal series are quite structured

but not too sharply; see (12) for a discussion). The range of singularities is not *a priori* bounded from above however, but in the experimental results it turned out to be so.

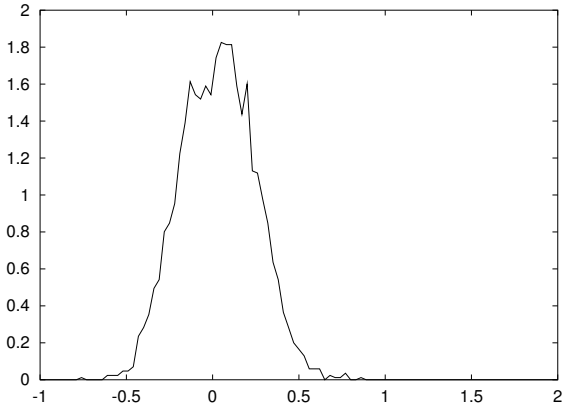

Fig. 4. Experimental distribution of h for Telefónica daily series

3.4 Log-normal vs log-Poisson statistics

The observed distribution of singularity exponents fits the log-Poisson model; on the contrary, it is incompatible with the log-normal model. Why? Because in the log-normal model the singularity exponents h are not bounded, neither from above nor from below. In Figure 5 we show a typical log-normal series. It was generated using the model presented in (22), and the parameters were

chosen to have a regular power spectrum and a reasonable dispersion. As it can be observed in Figure 5, log-normal series have sudden bursts which are extremely singular, but at the same time they are rather scarce (they correspond to events in the negative tail of the distribution of singularities). It is clear however from simple visual inspection that such a series does not resemble a real one due precisely to this unbounded bursts. The frequency of them is controlled by the dispersion of the gaussian, but they will eventually happen for a large enough data set.

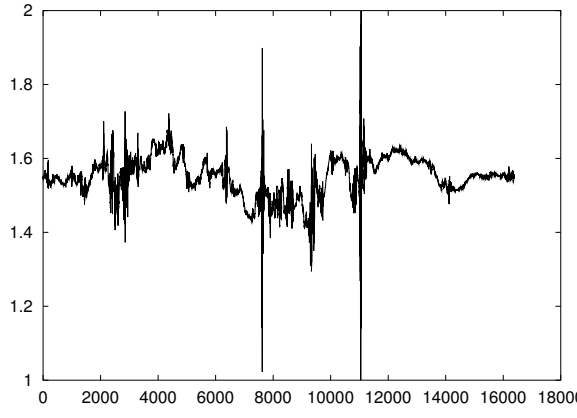

Fig. 5. A typical log-normal series. It was generated using the model in (22). The coeffients fit a log-normal of log-mean 0. and log-dispersion 0.5. The series contains 16384 points, and the basis wavelet is the second derivative of the gaussian.

This discrepancy with the behaviour of real series is also evidenced when the serie is analyzed using the geometrical approach. In Figure 6 we present the distribution of singularity exponents associated to the log-normal series in Figure 5. It assigns a non-null probability to extremely negative singularity exponents (which correspond to the bursts), which is physically unreasonable but characteristic of an unbounded distribution of singularities as the log-normal one. In contrast, singularities in real data are bounded, in agreement with the log-Poisson model. This boundness does not mean that the series is bounded (it could grow forever, for instance), but that there is no jump to infinity at any point.

However, multifractal stock series are quite often described in the scientific literature using log-normal statistics (for instance, in (23)). In such works the authors estimate the statistical self-similarity exponents from the data and make a quadratic fit (which corresponds to log-normal statistics) for some low-order moments . Finer analysis, as the one shown in (10), show a considerable deviation from the log-normal model for larger moments (which are precisely the ones dominated by the most singular exponents). What actually happens is that log-Poisson is indeed approximated *in law* by a log-normal as a consequence of Central Limit Theorem when the scale change is large enough. But as this approximation is granted *in law*, just the most probable events are

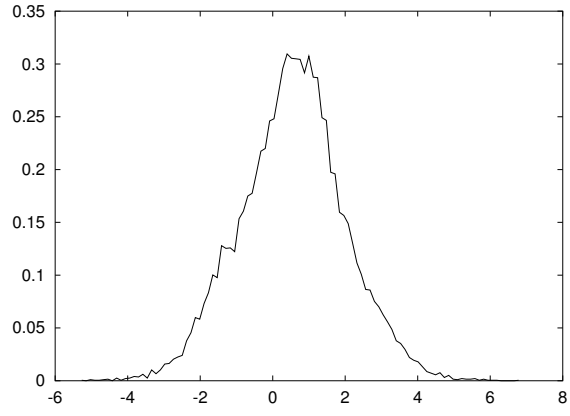

Fig. 6. Experimental distribution of h for the log normal series represented in Figure 5.

approximately equally distributed as in a log-normal model, while rare events (and specially the most singular events) are poorly described. Depending on the application, a log-normal model could be a good approximation or a very poor one. We will see in the following that in a geometrical picture it is precisely those rare events which allow to describe the whole series, and for that reason log-normal models are of no use in our context.

4 MSM and reconstruction

4.1 Theoretical background

Log-Poisson models are characterized by a very simple statistical feature: when an infinitesimally small change of scale takes place, just two events can happen: either the random variable changes smoothly or it undergoes a sudden change. The last possibility is interpreted as the crossing of one particular fractal component which concentrates the energy dissipation (in the case of turbulent flows) of the multifractal. A complete discussion about the statistics of log-Poisson multifractals and its interpretations would be quite extensive and somewhat pointless to be carried out here; the reader is referred to the wide bibliography on the subject. Let us cite here the basic works introducing the model and discussing its properties for turbulent flows (24; 25; 26; 27). For a discussion of the interplay between statistics and geometry and the relevance of log-Poisson statistics for multifractal descomposition, we refer to (12), in which the main questions are reviewed in a quite different context of application (the statistics of natural images).

According to (12), in log-Poisson multifractals there is a particular fractal component of maximum information content, the so called Most Singular Manifold (MSM). Log-Poisson statistics of changes in scale are characterized by the event of crossing or not that particular set. The MSM is defined as the fractal component associated to the least possible exponent h_∞ (that as we have seen verifies $-1 < h_\infty < 0$ for finite variation signals). We will denote shortly the MSM by $F_\infty \equiv F_{h_\infty}$. Due to the statistical interpretation of the MSM, in (28) it was proposed that a multifractal signal could be reconstructed from the values of the gradient over the MSM; as an hypothesis, it was stated that reconstruction is performed by means of a linear kernel. The kernel was uniquely determined under several reasonable requirements (isotropy, translational invariance and correspondence with the experimental power spectrum). We do not present here the whole derivation but the final expression; the reader is referred to the original paper. We will make use of the final formula to generalize it to the context of 1D series.

Let us start by defining the essential data needed to reconstruct. We will consider now a multifractal signal s defined over a multidimensional space, the points being identified by their vector coordinates $\vec{x}$. Hence, the signal will be given by the function $s(\vec{x})$. The multifractal measure μ is defined as the integral of $|\nabla s|(\vec{x})$, the modulus of the gradient, over the measured sets. The test of multifractality and singularity detection are carried out analogously to what was done for 1D signals. Let us define the essential gradient field,

$$\vec{v}(\vec{x}) \;\equiv\; \nabla s(\vec{x})\; \delta_{F_\infty}(\vec{x}) \tag{8}$$

where $\delta_{F_\infty}(\vec{x})$ is a delta-like function constant over the MSM F_∞ and vanishing outside that set. So, $\vec{v}$ contains all the information (geometry of the MSM and value of the measure over it) which we need to reconstruct, according to what is discussed in (28). As it is shown in that reference, the signal can be reconstructed using the following formula (expressed in the Fourier space):

$$\hat{s}(\vec{f}) \;=\; i\,\frac{\vec{f}\cdot\hat{\vec{v}}(\vec{f})}{f^2} \tag{9}$$

where hat ($\hat{}$) denotes Fourier transform, $\vec{f}$ is the frequency variable in the Fourier domain, i is the imaginary unit and the symbol " $\cdot$ " means scalar product of vectors. Let us notice that this formula has an interesting stability property: if we choose as F_∞ the total space, then $\vec{v} = \nabla s$, that is, $\hat{\vec{v}}(\vec{f}) = -i\vec{f}\hat{s}(\vec{f})$; substituting in eq. (9) we see that the equality is trivially satisfied. This means that there always exists a set (in the worst case, the whole space) from which reconstruction is perfect. A signal is reconstructible if there exists a smaller, rather sparse set F_∞ from which reconstruction is possible; or conversely, points not in F_∞ are predictable from those in F_∞.

The $1/f^2$ factor in eq. (9) creates a diffusion effect for signals in dimensions greater than 1, as this is the Fourier representation of a Green function associated to the Laplacian operator. A strong simplification appears when eq. (9) is applied to one-dimensional signals; then it reduces to:

$$\hat{s}(f) \;=\; i\frac{\hat{v}(f)}{f} \tag{10}$$

But i/f is a representation of the indefinite integral [4] , that is, an inverse of the derivative (as $\hat{s'}(f) = -if\hat{s}(f)$). So the reconstruction formula in 1D becomes:

$$s(t) \;=\; s(0) \;+\; \int_0^t d\tau\; v(\tau) \tag{11}$$

Let us make a few remarks on this formula. First, it has obviously the aforementioned stability property: if F_∞ is taken as the whole interval the formula is a trivial identity, as $v(t)$ becomes $s'(t)$ in such a case. Also, recalling that $v(t) = s'(t)\,\delta_{F_\infty}(t)$ we see that the weight of this function is concentrated in point-like contributions, in the points belonging to the MSM. For that reason, the series $s(t)$ obtained according to eq. (11) is piecewise constant, undergoing a change on its value when a point of the MSM is crossed.

Secondly, let us notice that eq. (11) does not imply that $s'(t) = 0$ for $t \notin F_\infty$. For continuous, ideal series, F_∞ is a dense set; therefore at any time t and any size ϵ there are points belonging to the MSM in $(t-\epsilon, t+\epsilon)$, and so $\int_{t-\epsilon}^{t+\epsilon} d\tau\; v(\tau)$ is non-vanishing in general. It follows that the derivative of the series $s(t)$ given in eq. (11) can be different from zero even at $t \notin F_\infty$.

On the contrary, over real, discretized data there is necessarily a loss in resolution: the integral in eq. (11) becomes a sum and the derivative is turned into the substraction of consecutive values; hence, the only points which can be removed in the sequence are those for which $s'(t) = 0$ strictly. However, at a given level of detail some points may be discarded without causing a great deviation between the reconstructed series and the real one. These points are obviously those for which the derivative is very small, but also other points in which the variations (derivatives) are significant but immediately compensated by changes of the opposite sign and similar absolute value. The key

[4] In the original derivation, the signal s had zero-mean to avoid divergence at zero frequency in eq. (9); for that reason the ambiguity in the choice of the constant is removed. In principle we assume that the integral of s over the considered time window is zero, what eliminates the ambiguity in the choice of the indefinite integral. We can change the convention to determine this constant, keeping consistency; in fact we have done it in eq. (11) by adding the term $s(0)$.

point is not the absolute value of the variations, but the resolution at which the series is described: significant variations are those which are large enough in comparison with those of the points nearby. At a given resolution, there will be an optimal set consisting of the points with the most significant changes. In fact, it is logical that the MSM could be identified with that set: it contains the points with the most negative exponents, that is, the points over which the transition (variation) is the sharpest. For those points the derivative is significantly greater than over the surrounding points (we will see in the following that the reconstruction out the MSM is rather good).

Determining the MSM is a rather standard procedure, much better than trying to assess by other means which points could be discarded when reconstructing. Calculating singularity exponents allows classifying the points according to the strength of the transition the series undergoes at them, giving a reasonable criterion to include or discard points in the MSM at a given precision, depending on the uncertainty or dispersion on the value h_∞. We will then use the MSM as minimum reconstructing set.

4.2 Experimental results and discussion

In Figure 7 we represent the reconstructed series for one daily and one minute sampling series; other series threw very similar results. In each case the MSM was determined via wavelet analysis as explained in Section 3; the MSMs were chosen as $h_\infty = -0.40 \pm 0.3$ (daily series) and $h_\infty = -0.45 \pm 0.3$ (minute series). The central value of h_∞ was determined as the average of the points associated to the 1% and the 5% left tails of the probability distribution of singularities h, as in (12). The uncertainty range (± 0.3) was conventionally fixed in such a way that the quality of the reconstruction was reasonable enough. As it is seen in Figure 7 the quality of the reconstruction is very good. According to eq. (11), the first point in the series has zero error and starting from it the error accumulates as time passes; for that reason the last point in the series is necessarily the worst predicted (in average). It is reasonable to proceed in such a way, as we deal with time series and one of the goals of this study is to make predictions and fluctuation estimation. Notice that the shape of the series is well captured by the reconstructed estimates, and errors mainly accumulate during very sharp transitions (specially for the periodic disruptions in minute series) which probably constitute a deviation from the multifractal description and should be treated separately. In spite of the presence of disruptive points in minute series, the reconstructed series provides good approximation. This is due to the fact that during a short period after a disruptive event (for instance, opening of NY market) the variations are larger than typical, but they keep

however the same multifractal arrangement, the MSM being still predictive. Just the very first instants fail to be described in the multifractal picture, and they are quite few. For that reason the present description is still valid in a good extent.

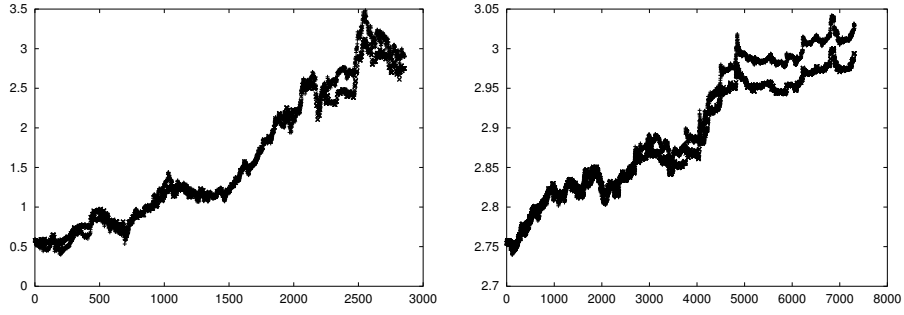

Fig. 7. Original (+) and reconstructed (x) (out the MSM) series for the daily series of Telefónica (left; PSNR for the reconstructed series: 27.86 dB) and for the one-minute series (right; PSNR: 24.64 dB)

For the chosen quantization in h_∞ (± 0.3), the density ρ_∞ of the MSM was always rather high ($\rho_\infty = 0.30$ for the daily series, $\rho_\infty = 0.29$ for the minute series). It could seem that the high quality of the reconstruction is just a consequence of the high value of the density for the MSM; however, if we replace the MSM in the reconstruction formula by uniform or random sampling with the same density, the quality is much lower (see Figures 8 and 9). This fact shows that the MSM has a large information content. Besides, the series obtained for those non-structured samplings have not a well defined tendency (they are not clearly, or not as much as the original series, increasing or decreasing). This implies that positive and negative variations are almost equally likely in price series: they are continuously oscillating. But, what is more surprising, the distributions of absolute values for positive and negative increments are quite similar. How to explain the tendency in the series?

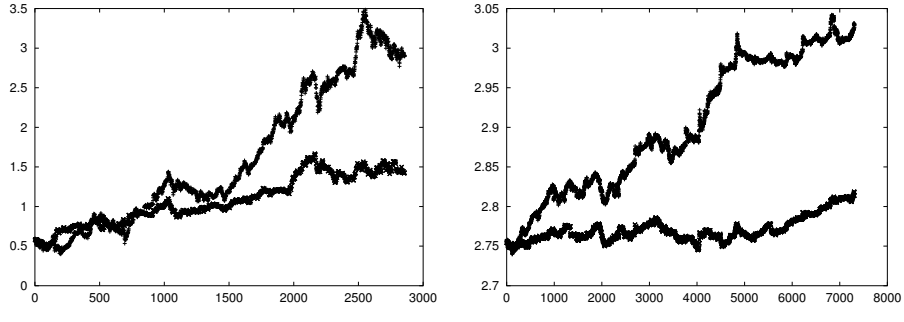

Fig. 8. Original (+) and reconstructed (x) (out a uniform sampling) series for Telefónica: daily (left; PSNR: 14.24 dB) and one-minute (right; PSNR: 12.03 dB)

Tendency changes just take place over the MSM, which is quite reduced in comparison to the total amount of points. Over the MSM, the distributions of positive and negative increments are still quite similar. However, the amount

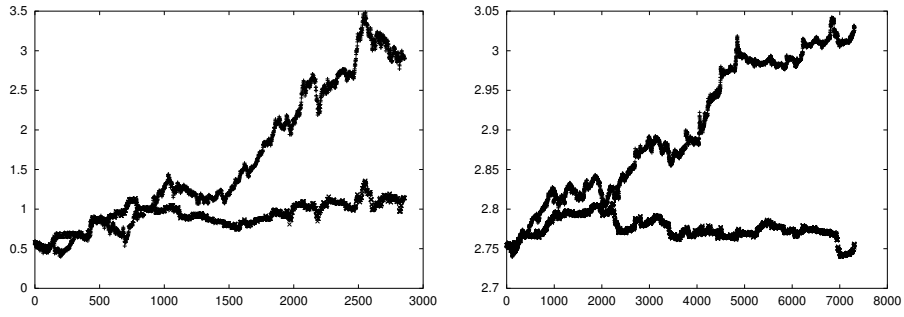

Fig. 9. Original (+) and reconstructed (x) (out a random sampling) series for Telefónica: daily (left; PSNR: 12.09 dB) and one-minute (right; PSNR: 10.50 dB)

of positive increments is greater (vs. smaller) than that of the negative ones for increasing (vs. decreasing) series; they are of the same order for no tendency series. For that reason, what determines the tendency of the series is not the absolute values of its increments, but the difference in number of positive and negative increments over the MSM. It is now obvious that tendency is difficult to assess with a sampling independent of the MSM. For instance, a random or uniform sampling of the whole series at 0.30 density would just sample 30% of MSM points, giving rise to a series with 30% as much tendency as the original one. To end the discussion, just remark that the characterization of the MSM as the set of tendency points is another way to express that MSM points are the most singular, the most significant with respect to their surroundings. Points outside the MSM are surrounded by similar, opposed tendency points, giving rise to a vanishing change in tendency.

We have shown that the MSM plays a fundamental role in the dynamics of the temporal series; ideally the series is fully described using this skeleton, this essential set. According to the reconstruction formula, eq. (11), and the definition of the essential gradient, eq. (8) (for 1D in our case), there are two different types of information which are needed to reconstruct, namely the geometry of the MSM (given by $\delta_{F_\infty}(t)$) and the values of the derivative s' on MSM. In the next section we will try to describe the dynamics governing the geometrical arrangement of the MSM; we leave the study of the intensities of the derivatives for a future work.

5 Dynamics on the MSM

Let us first define the MSM oriented density function, $\delta^o_{F_\infty}(t)$, which is given

by:

$$\delta^o_{F_\infty}(t) \;=\; \begin{cases} \delta_{F_\infty}(t) \;\; \text{if} \;\; t \in F_\infty \;,\; s'(t) > 0 \\ -\delta_{F_\infty}(t) \;\; \text{if} \;\; t \in F_\infty \;,\; s'(t) < 0 \\ 0 \qquad \text{if} \;\; t \notin F_\infty \end{cases} \tag{12}$$

So the orientated density function keeps the sign of the derivative on the MSM. This function keeps the information about the geometry of the MSM (as $|\delta^0_{F_\infty}| = \delta_{F_\infty}$), and at the same time it already incorporates some basic information about the derivative (its sign). This sign weighting is necessary to allow the possibility of cancellations when resolution is changed. Besides, as it was discussed in the previous section, the proportion of signs determines the tendency of the series [5] . In some sense, the function $\delta^o_{F_\infty}$ defines a naif series in which every event (non-zero value) means a relative change in the price of shares of the same absolute value. For that reason, a good understanding of the dynamics of this function could be useful to device a naif sell-buy model capable to produce correct multifractal exponents (that is, the statistics of changes in scale). For this analysis, we took averages over the two ensembles of data, assuming mutual statistical consistency among the different series they consisted of.

We tried first to identify two-point dependencies in $\delta^o_{F_\infty}$. We computed the mutual information between $\delta^o_{F_\infty}(t)$ and $\delta^o_{F_\infty}(t+\tau)$ for different time delays τ; assuming stationary statistics we disregard the basis points t. The generic value of $\delta^o_{F_\infty}(t)$ at any point will be denoted by σ, which can take the values -1, 1 or 0, depending if t belongs to the MSM with negative derivative, if t belongs to the MSM with positive derivative, or if t does not belong to the MSM, respectively. We adopt the following convention: a subscript τ associated to a state σ (i.e., σ_τ) indicates that the state takes place at a point which is displaced τ units with respect to a generic base point. We calculated the two-point joint probability as:

$$P(\sigma_0, \sigma_\tau) \;=\; \Big\langle \, \text{Prob}(\, \delta^o_{F_\infty}(t) = \sigma_0, \delta^o_{F_\infty}(t+\tau) = \sigma_\tau \,) \, \Big\rangle_t \tag{13}$$

[5] In fact the oriented density possesses stronger features: it defines (via the reconstruction formula) a multifractal series with the same singularity exponents as the original series. Its analysis will deserve future works.

and the marginal probability as:

$$P(\sigma) \;=\; \Big\langle\, \mathrm{Prob}(\, \delta^{o}_{F_\infty}(t) = \sigma \,) \,\Big\rangle_t \;\;=\;\; \langle P(\sigma, \sigma_\tau) \rangle_{\sigma_\tau} \quad \text{for any } \sigma_\tau \tag{14}$$

The mutual information between the points of the oriented MSM I_τ is then given by:

$$I_\tau = \sum_{\sigma_0=-1,0,1} \; \sum_{\sigma_\tau=-1,0,1} P(\sigma_0, \sigma_\tau) \; \log_2 \frac{P(\sigma_0, \sigma_\tau)}{P(\sigma_0) P(\sigma_\tau)} \tag{15}$$

that is, the Kullback distance between the joint probability $P(\sigma_0, \sigma_\tau)$ and the product of the marginal probabilities $P(\sigma_0)P(\sigma_\tau)$ (29); it is expressed in bits. It equals the entropy when the two variables are identical and vanishes only when they are independent; for that reason it is a good measure of statistical dependency. In Figure 10 we present the graphs of I_τ for both ensembles.

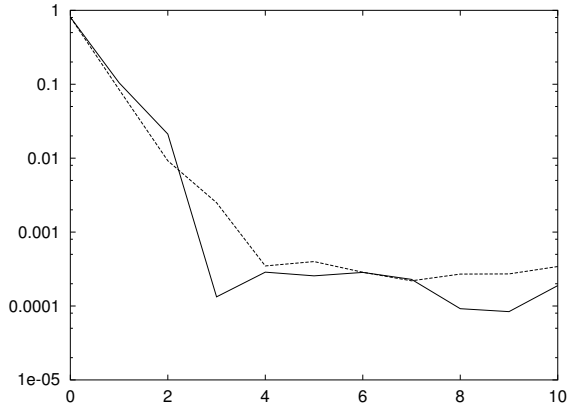

Fig. 10. Mutual information I_τ in semi-log plot for daily ensemble (continuous line) and one-minute ensemble (dashed)

Results for both ensembles are comparable. The mutual information I_τ decays extremely fast with the time displacement τ, so that at three time units of distance it is already negligible (comparable with the sampling uncertainty). This means that points in the MSM separated by such a distance can be considered independent. We would like to provide a stationary random process able to describe correctly this behaviour.

We propose that the joint probability $P(\sigma_0, \sigma_\tau)$ is obtained by τ successive applications of an elementary transition matrix $\mathbf{T}$ on $P(\sigma_0)$ (in fact this means that the random process is a Markov chain). In this model long range dependencies are a consequence of successive one-unit dependencies. Let us use $P(\sigma_0, \sigma_2)$ as an example. We can express it as:

$$P(\sigma_0, \sigma_2) \;=\; P(\sigma_2 | \sigma_0)\, P(\sigma_0) \tag{16}$$

where $P(\sigma_\tau|\sigma_0)$ stands for the conditional probability of obtaining the state σ_τ at the point at τ units of distance once the state at the base point is fixed to σ_0. Let us expand the conditional probability in terms of the intermediate state σ_1; we obtain:

$$P(\sigma_0, \sigma_2) \;=\; \sum_{\sigma_1} P(\sigma_2, \sigma_1|\sigma_0)\, P(\sigma_0) \tag{17}$$

Conditioning with respect to σ_1 it is obtained:

$$P(\sigma_0, \sigma_2) \;=\; \sum_{\sigma_1} P(\sigma_2|\sigma_1, \sigma_0)\, P(\sigma_1|\sigma_0)\, P(\sigma_0) \tag{18}$$

We assume that the random process is a stationary Markov chain, what means $P(\sigma_2|\sigma_1, \sigma_0) = P(\sigma_2|\sigma_1)$. Applying it to the previous expression:

$$P(\sigma_0, \sigma_2) \;=\; \sum_{\sigma_1} P(\sigma_2|\sigma_1)\, P(\sigma_1|\sigma_0)\, P(\sigma_0) \tag{19}$$

and comparing with eq. (16) we obtain the final formula for the random process:

$$P(\sigma_2|\sigma_0) \;=\; \sum_{\sigma_1} P(\sigma_2|\sigma_1)\, P(\sigma_1|\sigma_0) \tag{20}$$

that is, $P(\sigma_2|\sigma_0)$ is obtained by two applications of the random process described by $P(\sigma_1|\sigma_0)$. Let us introduce a matricial notation. We will represent the random process by a 3×3 matrix given by:

$$\mathbf{T} \;=\; \begin{pmatrix} t_{00} & t_{0+} & t_{0-} \\ t_{+0} & t_{++} & t_{+-} \\ t_{-0} & t_{-+} & t_{--} \end{pmatrix} \tag{21}$$

where $t_{\sigma_1\sigma_0} \equiv P(\sigma_1|\sigma_0)$. The matrix $\mathbf{T}$ defines the random process. With this notation eq. (20) can be rewritten as:

$$P(\sigma_2|\sigma_0) \;=\; \sum_{\sigma_1} t_{\sigma_2\sigma_1}\, t_{\sigma_1\sigma_0} \;\;=\;\; \mathbf{T}^2_{\sigma_2\sigma_0} \tag{22}$$

that is, the conditional distribution $P(\sigma_2|\sigma_0)$ is given by the square of the matrix $\mathbf{T}$. In general we obtain that at τ time units the matrix $\mathbf{T}^\tau$ is applied.

To test our hypothesis, we have compared the experimental $P(\sigma_0, \sigma_2)$ with that provided by eq. (19). The results are summarized in Tables 3 and 6. The

analysis of the results show that the hypothesis of Markovianity of the random process holds in a very good extent. We conclude that to the experimental extent the Markovian hypothesis is a reasonable first order approximation.

	$\sigma = 0$	$\sigma = 1$	$\sigma = -1$
P	0.71	0.16	0.13

Table 1
$P(\sigma)$ for daily ensemble. As $P(\sigma = +1) > P(\sigma = -1)$ the series exhibit an increasing tendency

	$\sigma_1 = 0$	$\sigma_1 = 1$	$\sigma_1 = -1$
$\sigma_0 = 0$	0.77	0.12	0.11
$\sigma_0 = 1$	0.54	0.43	0.03
$\sigma_0 = -1$	0.57	0.05	0.38

Table 2
Transition matrix $\mathbf{T}$ for daily ensemble

	$\sigma_1 = 0$	$\sigma_1 = 1$	$\sigma_1 = -1$
$\sigma_0 = 0$	0.51	0.11	0.09
$\sigma_0 = 1$	0.11	0.04	0.01
$\sigma_0 = -1$	0.09	0.01	0.03

	$\sigma_1 = 0$	$\sigma_1 = 1$	$\sigma_1 = -1$
$\sigma_0 = 0$	0.49	0.12	0.09
$\sigma_0 = 1$	0.12	0.04	0.01
$\sigma_0 = -1$	0.09	0.01	0.03

Table 3
$P(\sigma_0, \sigma_2)$ for daily ensemble. Top: Theoretical (according to eq. (19)); bottom: experimental

	$\sigma = 0$	$\sigma = 1$	$\sigma = -1$
P	0.70	0.20	0.10

Table 4
$P(\sigma)$ for one-minute ensemble. As $P(\sigma = +1) > P(\sigma = -1)$ the series exhibit an increasing tendency

6 Stability of the random process

	$\sigma_1 = 0$	$\sigma_1 = 1$	$\sigma_1 = -1$
$\sigma_0 = 0$	0.77	0.13	0.10
$\sigma_0 = 1$	0.53	0.44	0.03
$\sigma_0 = -1$	0.50	0.21	0.29

Table 5
Transition matrix $\mathbf{T}$ for one-minute ensemble

	$\sigma_1 = 0$	$\sigma_1 = 1$	$\sigma_1 = -1$
$\sigma_0 = 0$	0.49	0.13	0.07
$\sigma_0 = 1$	0.13	0.06	0.02
$\sigma_0 = -1$	0.07	0.02	0.01

	$\sigma_1 = 0$	$\sigma_1 = 1$	$\sigma_1 = -1$
$\sigma_0 = 0$	0.49	0.13	0.07
$\sigma_0 = 1$	0.13	0.06	0.02
$\sigma_0 = -1$	0.07	0.02	0.01

Table 6
$P(\sigma_0, \sigma_2)$ for one-minute ensemble. Top: Theoretical (according to eq. (19)); bottom: experimental

Let us analyze the stability of the random process associated to $\mathbf{T}$. We will represent the marginal probability by a three-dimensional vector $\vec{p} = (p_0, p_+, p_-)$ where $p_\sigma \equiv P(\sigma)$. Let us notice that $t_{\sigma'\sigma} p_\sigma = P(\sigma_0 = \sigma, \sigma_1 = \sigma')$, that is, the joint distribution of states separated a distance of one time unit. For that reason and using stationarity,

$$\sum_\sigma t_{\sigma'\sigma} p_\sigma \;=\; p_{\sigma'} \tag{23}$$

that is,

$$\mathbf{T}\vec{p} \;=\; \vec{p} \tag{24}$$

Eq. (24) has a great importance for the stability of the process: it means that the marginal probability distribution $\vec{p}$ is stable under application of the random process $\mathbf{T}$. Also, $\vec{p}$ is a eigenvector (of eigenvalue 1) of the matrix $\mathbf{T}$. A successive, iterative application of $\mathbf{T}$ over any distribution function would tend to make it more and more approximate to $\vec{p}$ as the process is applied. In fact, we should obtain all the eigenvalues of the matrix to make sure that the

largest one is precisely that associated to $\vec{p}$, which would make this point an attractor of the dynamics.

We have computed the eigenvalues associated to the random matrices $\mathbf{T}$ associated to both ensembles; we have represented them in Table 7, from the largest absolute value to the smallest one, for both ensembles

λ_1	λ_2	λ_3
1.00	0.36	0.20
1.00	$0.25 + 0.04i$	$0.25 - 0.04i$

Table 7
Eigenvalues associated to the random process. Top: daily ensemble; bottom: one-minute ensemble. The small imaginary part in the eigenvalues of the second ensemble is probably a numerical artifact

We observe that the stationarity is well verified: there is actually an eigenvalue equal to 1, and its associated eigenvector is precisely $\vec{p}$, the marginal distribution. But more importantly, this eigenvalue is the greatest in absolute value, so it dominates the convergence in the long run. Also, the other eigenvalues are positive but smaller than 1, so the part they describe tends to vanish when the process is applied iteratively. We conclude that the experimental random processes are stable and they converge to the observed marginal distribution.

Hence, the elemental random process $\mathbf{T}$ governs the dynamics which generate the oriented MSM. It would be possible to use this matrix to create a new multifractal elemental series with the same statistics as the original one. Of course, in practice $\mathbf{T}$ can be non-stationary, but anyway the time scale of its variation should be rather large, as the factorization hypothesis seems very consistent. Another important remark is that the stationary marginal distribution is completely defined by $\mathbf{T}$ (it is the only normalized eigenvector of eigenvalue 1). But the growing (or decreasing) character of the series is driven by the excess (or lack) of positive signs with respect to the negative signs in the series defined by the oriented MSM. So, the elemental random process would not only generate multifractal series, but always with the same growing or decreasing character: tendency is constant. To take account changes in tendency, a study on the fluctuations in the elementary random matrix should be introduced.

7 Conclusions

In this paper we have shown that fluctuations of returns in stock market time

series show multifractal properties. This multifractal character is reflected in a definite geometry for the series, arranged around fractal components of characteristic power law behaviour under changes in scale. We have exploited further this geometry and we have experimentally shown that the most singular of the fractal components (that is, the one which is dominant when the scale is reduced) can be used to reconstruct the whole series to a good extent. This means that the information about the series is contained in this set and its dynamics is driven by it. It has a highly non-trivial structure (what questions claims of "lack of structure" for economics series), as can be seen for the poor performance of random and uniform sampling with the same density. Also, an important information about the dynamics generating the MSM can be deduced from the data: at least in a good first order approximation, this set is constructed as a result of a Markov chain random process, in which the state of the point (which characterizes if the point belongs to the MSM, and its orientation in this case) is only dependent on the state of the previous point. This random process could be considered as the basis event to describe the dynamics underlying the series.

Future directions that should be addressed concerns the stability and econometric interpretation of this elemental random process, as its performance in generating good multifractal series, even prediction. A different but important issue to be considered is the description of the actual intensity (gradient) profile on the MSM. In fact, it can be proven (as it will be shown in future works) that it follows a slow varying pattern with however very important events.

Acknowledgement

A. Turiel is financially supported by a postdoctoral grant from the INRIA. We thank Gérard Weisbusch and specially Jean-Pierre Nadal for their help and support in the elaboration of this work and their comments. We also thank Sociedad de Bolsas as well as Risklab-Madrid for providing the data and Mcyt (contract BFM2000-0626) for financial support.

References

[1] J. P. Bouchaud, M. Potters, Theory of Financial Risk, Cambridge University Press, Cambridge, 2000.
[2] R. N. Mantegna, H. E. Stanley, An introduction to Econophysics, Cambridge University Press, 1999.
[3] R. N. Mantegna, H. E. Stanley, Scaling behavior of an economic index, Nature 376 (1995) 46–49.

[4] S. Galluccio, G. Caldarelli, M. Marsili, Y.-C. Zhang, Scaling in currency exchange, Physica A 245 (1997) 423–436.
[5] B. B. Mandelbrot, The variation of certain speculative prices, Journal of Bussiness XXXVI (1963) 392–417.
[6] B. Mandelbrot, H. M. Taylor, On the distribution of stock price differences, Operations research 15 (1967) 1057–1062.
[7] R. N. Mantegna, H. Stanley, Turbulence and financial markets, Nature 376 (1996) 46–49.
[8] S. Ghashghaie, W. Breymann, J. Peinke, P. Talkner, Y. Dodge, Turbulent cascades in foreign exchange market, Nature 381 (1996) 767.
[9] F. Schmitt, D. Schertzer, S. Lovejoy, Multifractal fluctuations in finance, International Journal of Theoretical and Applied Finance 3 (2000) 361–364.
[10] Y. Fujiwara, H. Fujisaka, Coarse-graining and self-similarity of price fluctuations, Physica A 294 (2001) 439.
[11] A. Arneodo, Wavelet analysis of fractals: from the mathematical concepts to experimental reality, in: G. Erlebacher, M. Y. Hussaini, L. Jameson (Eds.), Wavelets. Theory and applications, ICASE/LaRC Series in Computational Science and Engineering, Oxford University Press, Oxford, 1996, p. 349.
[12] A. Turiel, N. Parga, The multi-fractal structure of contrast changes in natural images: from sharp edges to textures, Neural Computation 12 (2000) 763–793.
[13] I. Daubechies, Ten lectures on wavelets, CBMS-NSF Series in Ap. Math., Capital City Press, Montpelier, Vermont, 1992.
[14] A. Davis, A. Marshak, W. Wiscombe, Wavelet based multifractal analysis of non-stationary and/or intermittent geophysical signals, in: E. Foufoula-Georgiou, P. Kumar (Eds.), Wavelet Transforms in Geophysics, Academic Press, New York, 1994, pp. 249–298.
[15] B. B. Mandelbrot, A. Fisher, L. Calvet, A multifractal model of asset returns, Cowles Foundation Discussion Paper No. 1164 .
[16] A. Arneodo, J.-F. Muzy, D. Sornette, "direct" causal cascade in the stock market, European Physical Journal B 2 (1998) 277–282.
[17] Y. Liu, P. Gopikrishnan, P. Cizeau, M. Meyer, C.-K. Peng, H. E. Stanley, The statistical properties of the volatility of price fluctuations, Phys. Rev. E 60 (1999) 1390–1400.
[18] P. Gopikrishnan, V. Plerou, Y. Liu, L. A. N. Amaral, X. Gabaix, H. E. Stanley, Scaling and correlation in financial time series, Physica A 287 (2000) 362–373.
[19] A. Arneodo, F. Argoul, E. Bacry, J. Elezgaray, J. F. Muzy, Ondelettes, multifractales et turbulence, Diderot Editeur, Paris, France, 1995.
[20] A. Turiel, N. Parga, Multifractal wavelet filter of natural images, Physical Review Letters 85 (2000) 3325–3328.
[21] G. Parisi, U. Frisch, On the singularity structure of fully developed turbulence, in: M. Ghil, R. Benzi, G. Parisi (Eds.), Turbulence and Pre-

dictability in Geophysical Fluid Dynamics. Proc. Intl. School of Physics E. Fermi, North Holland, Amsterdam, 1985, pp. 84–87.

[22] R. Benzi, L. Biferale, A. Crisanti, G. Paladin, M. Vergassola, A. Vulpiani, A random process for the construction of multiaffine fields, Physica D 65 (1993) 352–358.

[23] J. F. Muzy, J. Delour, E. Bacry, Modelling fluctuations of financial time series: from cascade process to stochastic volatility model., Euro. Phys. Journal B 17 (2000) 537–548.

[24] B. Dubrulle, Intermittency in fully developed turbulence: Log-poisson statistics and generalized scale covariance, Physical Review Letters 73 (1994) 959–962.

[25] Z. S. She, E. Leveque, Universal scaling laws in fully developed turbulence, Physical Review Letters 72 (1994) 336–339.

[26] Z. S. She, E. C. Waymire, Quantized energy cascade and log-poisson statistics in fully developed turbulence, Physical Review Letters 74 (1995) 262–265.

[27] B. Castaing, The temperature of turbulent flows, Journal de Physique II 6 (1996) 105–114.

[28] A. Turiel, A. del Pozo, Reconstructing images from their most singular fractal manifold, IEEE Trans. on Im. Proc. 11 (2002) 345–350.

[29] T. M. Cover, J. A. Thomas, Elements of information theory, John Wiley, New York, 1991.